

# On the Correlations between Flavour Observables in Minimal $U(2)^3$ Models

Andrzej J. Buras and Jennifer Girrbach

Physik Department, TUM, D-85748 Garching, Germany  
TUM-IAS, Lichtenbergstr. 2a, D-85748 Garching, Germany

## Abstract

We point out a number of correlations between flavour observables present in a special class of models, to be called  $MU(2)^3$ , with an approximate global  $U(2)^3$  flavour symmetry, constrained by a minimal set of spurions governing the breakdown of this symmetry. In this framework only Standard Model (SM) operators are relevant in  $\Delta F = 2$  transitions. While the New Physics contributions to  $\varepsilon_K$  have the same pattern as in models with constrained Minimal Flavour Violation (CMFV), the CP-violation induced by  $B_{s,d}^0 - \bar{B}_{s,d}^0$  mixings can deviate from the one in the SM and CMFV models. But these deviations in the  $B_d^0$  and  $B_s^0$  systems are strictly correlated by the  $U(2)^3$  symmetry with each other. The most important result of our paper is the identification of a stringent triple  $S_{\psi K_S} - S_{\psi\phi} - |V_{ub}|$  correlation in this class of models that constitutes an important test for them and in this context allows to determine  $|V_{ub}|$  by means of precise measurements of  $S_{\psi K_S}$  and  $S_{\psi\phi}$  with only small hadronic uncertainties. We also find that  $MU(2)^3$  models can in principle accommodate both *positive* and *negative* values of  $S_{\psi\phi}$ , but in the latter case  $|V_{ub}|$  has to be found in the ballpark of its exclusive determinations and the particular  $MU(2)^3$  model must provide a 20% enhancement of  $|\varepsilon_K|$ . As in this class of models  $|\varepsilon_K|$  can only be enhanced, this requirement can in principle naturally be satisfied, although it depends on the model considered. We provide an example of a supersymmetric  $MU(2)^3$  model that appears to satisfy these requirements. We summarize briefly the pattern of flavour violation in rare  $K$  and  $B_{s,d}$  decays in  $MU(2)^3$  and compare it with the one found in CMFV models.

# 1 Introduction

The simplest class of extensions of the Standard Model (SM) are models with constrained MFV (CMFV) [1–3] that similarly to the SM imply stringent correlations between observables in  $K$ ,  $B_d$  and  $B_s$  systems, while allowing for significant departures from SM expectations. These correlations are consistent with present flavour data except possibly for the  $\Delta M_{s,d} - \varepsilon_K$  correlation, which appears to experience some tension [4]. However, improved lattice calculations of the relevant non-perturbative parameters and the reduction of the uncertainty in  $|V_{cb}|$  that enters  $\varepsilon_K$  as  $|V_{cb}|^4$  are necessary in order to firmly establish this result. Similar comments apply to the visible  $S_{\psi K_S} - \varepsilon_K$  tension [5, 6] within the SM.

Now most models with new sources of flavour and CP-violation can presently provide a better simultaneous description of  $\Delta M_{s,d}$ ,  $\varepsilon_K$  and  $S_{\psi K_S}$  than achieved within the SM and CMFV models. However, when no flavour symmetries are present in a given model, the pattern of deviations from SM and CMFV expectations is not always transparent.

The situation is quite different in possibly simplest non-MFV extensions of the SM based on a global  $U(2)^3$  flavour symmetry, rather than  $U(3)^3$  symmetry that governs CMFV [1] and MFV [7] models. This class of models studied in [8–13]<sup>1</sup> has several interesting features that allow to distinguish it from CMFV and MFV models. As discussed very recently in [16] the implications of  $U(2)^3$  symmetry for flavour physics depends on the way it is broken:

- In the so-called minimal  $U(2)^3$  models ( $MU(2)^3$ ), analyzed in [8–10] only the minimal set of spurions is used to break the flavour symmetry implying rather stringent relations between various flavour observables.
- When additional spurions are included in the so-called generic  $U(2)^3$  models ( $GU(2)^3$ ), as done in [16], the implications for flavour physics are less constrained but this is maybe necessary one day if  $MU(2)^3$  will be falsified by the future precise data.

Here we would like to reconsider the correlations between flavour observables in  $MU(2)^3$  models. As we will see below with respect to  $\Delta F = 2$  observables all models of this class can be parametrized by addition to the SM parameters of only *three* new parameters: one complex phase and two *real* and *positive definite* parameters of which one is restricted to be equal to or larger than unity.

We should already state at the beginning that our goal is not to demonstrate that the  $MU(2)^3$  models are consistent with the present data because this has been already shown in [8–10]. Partly this is due to existing hadronic, parametric and experimental uncertainties in flavour observables. Yet, these uncertainties will be significantly reduced in the coming years and it is of interest to ask how  $MU(2)^3$  models would face

---

<sup>1</sup>For earlier discussions of  $U(2)$  symmetry see [14, 15].

precision flavour data and the reduction of hadronic and CKM uncertainties. In this respect correlations between various observables are very important and we would like to exhibit these correlations by assuming reduced uncertainties in question. We will be more explicit about it in Section 4.

Now, the most interesting features that allow to distinguish  $MU(2)^3$  models from CMFV models are as follows:

- New CP-violating phases in  $B_d^0 - \bar{B}_d^0$  and  $B_s^0 - \bar{B}_s^0$  systems are present, thereby allowing for departures of the corresponding mixing induced CP-asymmetries  $S_{\psi K_S}$  and  $S_{\psi\phi}$  from the SM and CMFV values. However, very importantly, this appears in a correlated manner: the new phases  $\varphi_{B_d}$  and  $\varphi_{B_s}$  are forced by the  $U(2)^3$  symmetry to be equal<sup>2</sup>

$$\varphi_{B_d} = \varphi_{B_s}. \quad (1)$$

- The stringent CMFV correlations between K-physics observables and B-physics observables are generally absent in these models<sup>3</sup>, allowing among other things to avoid the  $\Delta M_{s,d} - \varepsilon_K$  tension mentioned above. This also means that even if NP effects in  $B_s$  and  $B_d$  meson system would be found to be very small one day, this would not necessarily imply, in contrast to CMFV models, small effects in rare  $K$  decays like  $K^+ \rightarrow \pi^+ \nu \bar{\nu}$  and  $K_L \rightarrow \pi^0 \nu \bar{\nu}$  and the ratio  $\varepsilon'/\varepsilon$ .
- On the other hand several relations involving CP-conserving observables in  $B_d$  and  $B_s$  meson systems known from CMFV models and also within the  $K$  system remain valid, even if individual predictions for these observables can significantly differ from those found in CMFV scenario. This applies in particular to  $\Delta M_{s,d}$  and  $B_{s,d} \rightarrow \mu^+ \mu^-$ .

Several of these properties have been already identified in the extensive work of Barbieri and collaborators [8–10]. Here we would like to point out another correlation in  $MU(2)^3$  flavour models, which to our knowledge has not been discussed in the literature so far:

- The triple correlation:

$$S_{\psi K_S} - S_{\psi\phi} - |V_{ub}|, \quad (2)$$

which as we will see below will provide a crucial test of the  $MU(2)^3$  scenario once the three observables will be precisely known. That is once the two of these observables are known, the third one is predicted in these models subject to small dependence on the angle  $\gamma$  and other uncertainties mentioned below.

- However, as far as  $\Delta F = 2$  are concerned, the models which pass this test should also simultaneously describe the data for  $\varepsilon_K$  and  $\Delta M_{s,d}$ .

<sup>2</sup>To our knowledge first discussions of this relation can be found in [17, 18].

<sup>3</sup>However, in specific models of this type some correlations between  $K$  and  $B$  physics could take place.

Presently [19, 20]

$$S_{\psi K_S}^{\text{exp}} = 0.679 \pm 0.020, \quad S_{\psi\phi}^{\text{exp}} = 0.002 \pm 0.087 \quad (3)$$

and improvements from the LHCb, ATLAS and CMS are expected in due time. These results confirm the general SM and CMFV expectations that mixing induced CP violation in  $B_d$  decays is much larger than in  $B_s$  decays.

On the other hand the situation with  $|V_{ub}|$  is unclear at present as its values extracted from exclusive and inclusive semi-leptonic B-decays differ significantly from each other: [19, 21]

$$|V_{ub}|_{\text{excl}} = (3.12 \pm 0.26) \times 10^{-3}, \quad |V_{ub}|_{\text{incl}} = (4.27 \pm 0.38) \times 10^{-3}. \quad (4)$$

For a recent discussion see [22].

Therefore the most sophisticated numerical analyses of NP effects in various extensions of the SM found in the literature use as input some kind of an average between the inclusive and exclusive determination of  $|V_{ub}|$ . For instance the authors of [8] use

$$|V_{ub}| = (3.97 \pm 0.45) \times 10^{-3}. \quad (5)$$

While such an approach is legitimate, it may hide some interesting physics behind the values of  $|V_{ub}|$  which are washed out in such an approach. Similar comments apply to the analyses in [23–25].

In this context we should emphasize that one of the recent highlights in particle physics was the measurement of the angle  $\theta_{13}$  in the PMNS matrix with a precision significantly larger than the corresponding precision on  $|V_{ub}|$ . The unexpectedly high value of  $\theta_{13}$  had a large impact on the models for the PMNS matrix and the field of lepton flavour violation. For recent reviews see [26, 27].

Now, as assured by various documents on future determinations of  $|V_{ub}|$  [28–30], the second half of this decade could bring also significant progress on  $|V_{ub}|$  and one can anticipate that this will also have an impact on the physics of quarks. Therefore, we have emphasized in recent papers [4, 31, 32] that the future precise determination of  $|V_{ub}|$  combined with a more accurate determination of the angle  $\gamma$  and reduced uncertainties in the hadronic parameters relevant for  $\Delta F = 2$  transitions by future lattice calculations, could already on the basis of a few  $\Delta F = 2$  observables distinguish uniquely between the simplest extensions of the SM. In this context we have considered two scenarios for  $|V_{ub}|$ :

- **Exclusive (small)  $|V_{ub}|$  Scenario 1:**  $|\varepsilon_K|$  is smaller than its experimental determination, while  $S_{\psi K_S}$  is rather close to the central experimental value.
- **Inclusive (large)  $|V_{ub}|$  Scenario 2:**  $|\varepsilon_K|$  is consistent with its experimental determination, while  $S_{\psi K_S}$  is significantly higher than its experimental value.

Thus dependently which scenario is considered we need either *constructive* NP contributions to  $|\varepsilon_K|$  (Scenario 1) or *destructive* NP contributions to  $S_{\psi K_S}$  (Scenario 2). However this NP should not spoil the agreement with the data for  $S_{\psi K_S}$  (Scenario 1) and  $|\varepsilon_K|$  (Scenario 2).

While introducing these two scenarios, one should emphasize the following difference between them. In Scenario 1, the central value of  $|\varepsilon_K|$  is visibly smaller than the very precise data but the still significant parametric uncertainty due to  $|V_{cb}|^4$  dependence in  $|\varepsilon_K|$  and a large uncertainty in the charm contribution found at the NNLO level in [33] does not make this problem as pronounced as this is the case of Scenario 2, where large  $|V_{ub}|$  implies definitely a value of  $S_{\psi K_S}$  that is by  $3\sigma$  above the data.

In the present paper we will generalize these considerations by including the full range

$$2.8 \times 10^{-3} \leq |V_{ub}| \leq 4.6 \times 10^{-3} \quad (6)$$

in our analysis and calculating how the correlation between  $S_{\psi K_S}$  and  $S_{\psi\phi}$  in  $MU(2)^3$  models depends on the value of  $|V_{ub}|$ , which hopefully will be known precisely one day.

Thus the main new result in the present paper is Fig. 1, which will allow us in the future to monitor how  $MU(2)^3$  models are facing the improved data on  $S_{\psi K_S}$ ,  $S_{\psi\phi}$  and  $|V_{ub}|$ . We would like to emphasize that hadronic uncertainties in  $S_{\psi K_S}$  and  $S_{\psi\phi}$  are presently significantly smaller than in  $\Delta M_{s,d}$  and  $\varepsilon_K$ , although we are aware of the possibility that in the era of precision flavour physics additional effects from QCD-penguin effects should be taken into account in the extraction of model parameters from these asymmetries [34–45].

Another new result in the context of  $MU(2)^3$  models, that follows from Fig. 1, is the realization that in these models  $S_{\psi\phi}$  can not only be smaller than the SM value but also have opposite sign. Here we differ from the authors of [8, 9] who using the  $|V_{ub}|$  in (5) concluded that a striking prediction of the  $U(2)^3$  framework is a value of  $S_{\psi\phi}$  in the range  $0.05 \leq S_{\psi\phi} \leq 0.20$  implying that a future *negative* value of  $S_{\psi\phi}$  would rule out this framework<sup>4</sup>. Fortunately as Fig. 1 demonstrates this is not the case. However this requires a rather low value of  $|V_{ub}|$ , in the ballpark of exclusive determinations, and consequently a positive contribution to  $|\varepsilon_K|$  of the order of 20%, which likely cannot be achieved in all  $MU(2)^3$  models. On the other hand an enhancement of  $|\varepsilon_K|$  similarly to CMFV is a unique, basically model independent, prediction of the  $MU(2)^3$  framework.

Another related correlation in this framework is the one between  $\mathcal{B}(B^+ \rightarrow \tau^+ \nu_\tau)$  and  $S_{\psi\phi}$  and given in Fig. 5 that in due time will constitute an important constraint on  $MU(2)^3$  models. We also point out that in an  $MU(2)^3$  flavour symmetric world one can determine  $|V_{ub}|$  by means of precise measurements of  $S_{\psi K_S}$  and  $S_{\psi\phi}$  with only small hadronic uncertainties.

---

<sup>4</sup>The same conclusion is reached in the 2HDM<sub>MFV</sub> framework [4, 46–48] but in this case no escape through a low value of  $|V_{ub}|$  is possible as in this model the contributions to  $\varepsilon_K$  are tiny.

Finally we point out that  $B_{s,d} \rightarrow \mu^+ \mu^-$  decays allow to test new CP-violating phases in  $MU(2)^3$  models with the help of mixing induced CP-asymmetries  $S_{\mu^+ \mu^-}^{s,d}$  proposed in [49, 50].

Our paper is organized as follows. In Section 2 we describe the departures from SM predictions for  $\Delta F = 2$  processes in terms of general expressions. In Section 3 we specify these expressions to CMFV models and  $MU(2)^3$  models. In Section 4 we present a general numerical analysis of  $\Delta F = 2$  observables in  $MU(2)^3$  models with the main results represented by Figs. 1–5 and the implications thereof. In Section 5 we outline a strategy for testing the  $MU(2)^3$  scenario in the coming years. Subsequently we execute this strategy in the case of a specific supersymmetric model of the  $MU(2)^3$  type. While a detailed sophisticated analysis of this model with the  $|V_{ub}|$  in (5) has been already presented in [8], we show that a more specific look at the values of  $|V_{ub}|$  allows to obtain some insight which goes beyond the results obtained by these authors. In Section 6 we summarize briefly the pattern of flavour violation in rare  $K$  and  $B_{s,d}$  decays in  $MU(2)^3$  models. A summary of our main results and a brief outlook for the future are given in Section 7.

## 2 Basic Formulae for $\Delta F = 2$ Observables

The expressions for the off-diagonal elements  $M_{12}^i$  in the neutral  $K$  and  $B_q$  meson mass matrices for the models considered in our paper can be written in a general form as follows

$$(M_{12}^K)^* = \frac{G_F^2}{12\pi^2} F_K^2 \hat{B}_K m_K M_W^2 [\lambda_c^2 \eta_1 x_c + \lambda_t^2 \eta_2 S_K + 2\lambda_c \lambda_t \eta_3 S_0(x_c, x_t)] , \quad (7)$$

$$(M_{12}^q)^* = \frac{G_F^2}{12\pi^2} F_{B_d}^2 \hat{B}_{B_d} m_{B_d} M_W^2 \left[ \left( \lambda_t^{(q)} \right)^2 \eta_B S_q \right] , \quad (8)$$

where  $q = d, s$ ,  $x_i = m_i^2/M_W^2$  and

$$\lambda_i^{(K)} = V_{is}^* V_{id}, \quad \lambda_t^{(q)} = V_{tb}^* V_{tq} \quad (9)$$

with  $V_{ij}$  being the elements of the CKM matrix. Here,  $S_0(x_c, x_t)$  is a *real valued* one-loop box function for which explicit expression is given e. g. in [51]. The factors  $\eta_i$  are QCD corrections evaluated at the NLO level in [52–56]. For  $\eta_1$  and  $\eta_3$  also NNLO corrections have been recently calculated [33, 57]. Finally  $\hat{B}_K$  and  $\hat{B}_{B_q}$  are the well-known non-perturbative factors.

In the  $MU(2)^3$  framework of [8], similarly to MFV, NP enters these expressions only in terms proportional to  $\lambda_t^{(K)}$  and  $\lambda_t^{(q)}$ , that is through the functions  $S_i$  with  $i = K, q$ . But this time these functions can be complex:

$$S_i \equiv |S_i| e^{i\theta_i^s} . \quad (10)$$

Note that the flavour dependence enters the mixing amplitudes through the elements of the CKM matrix and the functions  $S_i$  in question. We emphasize the complex conjugation in the expressions for mixing amplitudes, which is essential as  $S_i$  beyond the SM and CMFV carry in principle new complex phases.

The  $\Delta B = 2$  mass differences can now be written as follows:

$$\Delta M_d = 2|M_{12}^d| = \frac{G_F^2}{6\pi^2} M_W^2 m_{B_d} |\lambda_t^{(d)}|^2 F_{B_d}^2 \hat{B}_{B_d} \eta_B |S_d|, \quad (11)$$

$$\Delta M_s = 2|M_{12}^s| = \frac{G_F^2}{6\pi^2} M_W^2 m_{B_s} |\lambda_t^{(s)}|^2 F_{B_s}^2 \hat{B}_{B_s} \eta_B |S_s|. \quad (12)$$

The corresponding mixing induced CP-asymmetries are then given by

$$S_{\psi K_S} = \sin(2\beta + 2\varphi_{B_d}), \quad S_{\psi\phi} = \sin(2|\beta_s| - 2\varphi_{B_s}), \quad (13)$$

where the phases  $\beta$  and  $\beta_s$  are defined by

$$V_{td} = |V_{td}|e^{-i\beta}, \quad V_{ts} = -|V_{ts}|e^{-i\beta_s}. \quad (14)$$

$\beta_s \simeq -1^\circ$ . The new phases  $\varphi_{B_q}$  are directly related to the phases of the functions  $S_q$ :

$$2\varphi_{B_q} = -\theta_S^q. \quad (15)$$

For the CP-violating parameter  $\varepsilon_K$  we have

$$\varepsilon_K = \frac{\kappa_\varepsilon e^{i\varphi_\varepsilon}}{\sqrt{2}(\Delta M_K)_{\text{exp}}} [\Im(M_{12}^K)], \quad (16)$$

where  $\varphi_\varepsilon = (43.51 \pm 0.05)^\circ$  and  $\kappa_\varepsilon = 0.94 \pm 0.02$  [6, 58] takes into account that  $\varphi_\varepsilon \neq \frac{\pi}{4}$  and includes long distance effects in  $\Im(\Gamma_{12})$  and  $\Im(M_{12})$ .

In the rest of the paper, unless otherwise stated, we will assume that all four parameters in the CKM matrix have been determined through tree-level decays without any NP pollution and pollution from QCD-penguin diagrams so that their values can be used universally in all NP models considered by us.

### 3 CMFV vs. $MU(2)^3$ Models: $\Delta F = 2$ Observables

The  $\Delta F = 2$  observables discussed above can be calculated in any model by specifying the functions  $S_i$ <sup>5</sup>. Before doing it here, let us summarize briefly the basics of these two classes of extensions of the SM.

---

<sup>5</sup>Note, that this statement applies also to models with new operators as their contributions can always be included in the definition of  $S_i$  but then these functions will depend on new non-perturbative parameters.

### 3.1 Constrained Minimal Flavour Violation (CMFV)

This is possibly the simplest class of BSM scenarios. It is defined pragmatically as follows [1]:

- The only source of flavour and CP violation is the CKM matrix. This implies that the only CP-violating phase is the KM phase and that CP-violating flavour blind phases are assumed to be absent.
- The only relevant operators in the effective Hamiltonian below the electroweak scale are the ones present within the SM.

Detailed expositions of phenomenological consequences of this NP scenario has been given in [2, 3] and recently in [4]. The main implications of this framework are listed below.

In the grander formulation by means of effective theory approach [7], CMFV corresponds to the case of one Higgs doublet and the pragmatic assumption that no new operators beyond those present in the SM at the electroweak scale are relevant. This assumption is useful as finding the departures from CMFV could also point out to new operators and/or new sources of flavour violation.

### 3.2 Minimal $U(2)^3$ Models

A pragmatic definition of these models in the case of  $\Delta F = 2$  transitions could be as follows:

- Flavour and CP-violation in the  $\Delta S = 2$  transitions is governed by CMFV.
- The dominant source of flavour and CP violation in  $B_{d,s} - \bar{B}_{d,s}$  mixings is the CKM matrix. Yet, new universal, with respect to  $B_d$  and  $B_s$ , flavour violating and CP-violating effects in these transitions are possible. The universality in question is a direct consequence of the  $U(2)^3$  symmetry imposed on the quark doublets of the first two generations. Moreover, only SM operators are relevant in  $B_{d,s} - \bar{B}_{d,s}$  mixings. We comment on the possible small non-universal corrections and contributions of new operators below.
- Very importantly NP effects in  $K$  physics and  $B_{d,s}$  observables are uncorrelated with each other, although in specific models such correlation could be forced by the underlying theory and the data.

In the grander formulation by means of effective theory [8] these models are governed by a global flavour symmetry

$$G_F = U(2)_Q \times U(2)_u \times U(2)_d \quad (17)$$

broken *minimally* by three spurions transforming under  $G_F$  as follows

$$\Delta Y_u = (2, \bar{2}, 1), \quad \Delta Y_d = (2, 1, \bar{2}), \quad V = (2, 1, 1). \quad (18)$$

As demonstrated by means of a spurion analysis in Section 5 of [8], the phenomenological consequences of this framework for  $\Delta F = 2$  transitions as summarized in the pragmatic definition are general consequences of  $U(2)^3$  symmetry and its breaking pattern. They go beyond supersymmetry that otherwise dominates this paper. In particular, if one considers leading flavour-changing amplitudes no assumption of the dominance of SM operators has to be made. Moreover, the universality of NP effects in  $B_{d,s} - \bar{B}_{d,s}$  systems, up to the overall usual CKM factors and the hermicity of the  $\Delta F = 2$  Hamiltonian implies that  $S_K$  is real [8]. This result in combination with the dominance of SM operators in this framework implies the CMFV structure of  $\Delta S = 2$  transitions.

In this context the following remark should be made. As in the MFV framework the leading flavour-changing amplitudes in the framework of [8] are of left-handed type and to a very good approximation can be evaluated neglecting the effects of light-quark masses. In order to generate dimension six LR operators contributing to  $\Delta F = 2$  transitions one needs at least two extra insertion of the down-type spurion  $\Delta Y_d$  which implies an extra suppression of amplitudes proportional to down-quark masses. Such effects being proportional to light quark masses ( $m_{s,d}$ ) break the flavour universality between  $B_d$  and  $B_s$  systems and introduce corrections to the relation (1). They can be at best relevant for  $B_s$ -mixing, for instance in 2HDM models or supersymmetric models. However, unless one goes to a specific regime of large  $\tan\beta$  and small Higgs masses such effects are always subleading and we will neglect them.

More interesting in this context are the operators

$$Q_1^{\text{SLL}} = (\bar{b}P_L s) (\bar{b}P_L s), \quad Q_2^{\text{SLL}} = (\bar{b}\sigma_{\mu\nu}P_L s) (\bar{b}\sigma^{\mu\nu}P_L s) \quad (19)$$

present in the  $2\text{HDM}_{\overline{\text{MFV}}}$  framework [4, 46–48]. Having Wilson coefficients proportional to  $m_b^2$ , their contributions have the same impact on  $B_s$  and  $B_d$  mixings and satisfy in particular the relation (1). In [47] they correspond to the dominance of flavour blind phases in the Higgs potential, rather than to such phases in Yukawa couplings corresponding to LR operators and considered in [46]. In fact our statements on  $2\text{HDM}_{\overline{\text{MFV}}}$  in the present paper apply only to the case of the dominance of the operators in (19) as only in this case the  $2\text{HDM}_{\overline{\text{MFV}}}$  framework has a chance to remove the  $\varepsilon_K - S_{\psi\phi}$  tension in the SM. However, to generate such operators in the  $2\text{HDM}_{\overline{\text{MFV}}}$  framework requires not only flavour blind phases but also sizable  $SU(2)_L$  breaking in the Higgs potential (splitting between  $m_A$  and  $m_H$ ). Finally the contributions of the operators in (19) to  $\Delta S = 2$  are proportional to  $m_s^2$  and negligible.

### 3.3 Comparison

For our purposes it will be sufficient to discuss first only those general properties of the  $S_i$  in these two NP scenarios from which correlations between various observables

automatically follow. We have then:

1. In CMFV we have

$$S_K = S_d = S_s \geq S_0(x_t), \quad \varphi_K = \varphi_{B_d} = \varphi_{B_s} = 0, \quad (\text{CMFV}) \quad (20)$$

where  $S_0(x_t)$  is the SM box function given by

$$S_0(x_t) = \frac{4x_t - 11x_t^2 + x_t^3}{4(1-x_t)^2} - \frac{3x_t^2 \log x_t}{2(1-x_t)^3} \quad (21)$$

and the inequality in (20) has been demonstrated diagrammatically in [59]. Consequently

$$S_{\psi K_S} = \sin(2\beta), \quad S_{\psi\phi} = \sin(2|\beta_s|) \quad (\text{CMFV}). \quad (22)$$

$|\varepsilon_K|$ ,  $\Delta M_d$  and  $\Delta M_s$  can only be enhanced in CMFV models. Moreover, this happens in a correlated manner. The enhancement of one of these observables implies automatically and uniquely the enhancement of the other two observables [3, 60].

2. On the other hand in  $MU(2)^3$  models (20) and (22) are replaced by

$$S_K = r_K S_0(x_t), \quad |S_d| = |S_s| = r_B S_0(x_t), \quad \varphi_K = 0, \quad \varphi_{B_d} = \varphi_{B_s} \equiv \varphi_{\text{new}}, \quad (\text{MU}(2)^3) \quad (23)$$

and consequently

$$S_{\psi K_S} = \sin(2\beta + 2\varphi_{\text{new}}), \quad S_{\psi\phi} = \sin(2|\beta_s| - 2\varphi_{\text{new}}), \quad (\text{MU}(2)^3) \quad (24)$$

implying a correlation between these two asymmetries. As there is no relation of  $S_d = S_s$  to the SM box function  $S_0(x_t)$  and  $S_K$  in these models,  $\Delta M_d$  and  $\Delta M_s$  can be suppressed or enhanced with respect to the SM values and there is no direct correlation between  $|\varepsilon_K|$  and  $\Delta M_{s,d}$ .

In short, with respect to  $\Delta F = 2$  processes there are only three new parameters in this class of models

$$r_K \geq 1, \quad r_B, \quad \varphi_{\text{new}} \quad (25)$$

with  $r_K$  and  $r_B$  being real and positive definite.

The first inequality in (25) is a direct consequence of the CMFV structure in the  $\Delta S = 2$  transitions in this framework [59]. Therefore in the  $MU(2)^3$  framework  $|\varepsilon_K|$  can only be increased over the SM value, which is supported by the data but as stated above, this property is generally uncorrelated with  $B_{s,d}$  systems.

3. The flavour universality of the functions  $S_q$  in CMFV and  $MU(2)^3$  models implies

$$\left( \frac{\Delta M_d}{\Delta M_s} \right)_{\text{CMFV}} = \left( \frac{\Delta M_d}{\Delta M_s} \right)_{\text{MU}(2)^3} = \left( \frac{\Delta M_d}{\Delta M_s} \right)_{\text{SM}} = \frac{m_{B_d} \hat{B}_d F_{B_d}^2}{m_{B_s} \hat{B}_s F_{B_s}^2} \left| \frac{V_{td}}{V_{ts}} \right|^2 \equiv \frac{m_{B_d}}{m_{B_s}} \frac{1}{\xi^2} \left| \frac{V_{td}}{V_{ts}} \right|^2. \quad (26)$$

The  $\Delta F = 1$  observables are discussed in Section 6.

## 4 General Numerical Analysis

### 4.1 Strategy

As we stated at the beginning of our paper it is not the goal of this section to present a full-fledged numerical analysis of all correlations including present theoretical and experimental uncertainties as this would only wash out the effects we want to emphasize. We think that in view of the flavour precision era ahead of us it is more important to identify certain characteristic features of this NP scenario by decreasing present hadronic and parametric uncertainties. Therefore, in our numerical analysis we will choose as nominal values for three out of four CKM parameters:

$$|V_{us}| = 0.2252, \quad |V_{cb}| = 0.0406, \quad \gamma = 68^\circ, \quad (27)$$

where the values for  $|V_{us}|$  and  $|V_{cb}|$  have been measured in tree level decays. The value for  $\gamma$  is consistent with CKM fits and as the ratio  $\Delta M_d/\Delta M_s$  in the model considered equals the SM one, this choice is a legitimate one. Indeed the SM value for this ratio agrees well with the data. Other inputs are collected in Table 1. For  $|V_{ub}|$  we will use the range in (6).

Having fixed the three parameters of the CKM matrix to the values in (27), for a given  $|V_{ub}|$  the “true” values of the angle  $\beta$  and of the element  $|V_{td}|$  are obtained from the unitarity of the CKM matrix:

$$|V_{td}| = |V_{us}||V_{cb}|R_t, \quad R_t = \sqrt{1 + R_b^2 - 2R_b \cos \gamma}, \quad \cot \beta = \frac{1 - R_b \cos \gamma}{R_b \sin \gamma}, \quad (28)$$

where

$$R_b = \left(1 - \frac{\lambda^2}{2}\right) \frac{1}{\lambda} \frac{|V_{ub}|}{|V_{cb}|}. \quad (29)$$

In Table 2 we summarize for completeness the SM results for  $|\varepsilon_K|$ ,  $\Delta M_{s,d}$ ,  $(\sin 2\beta)_{\text{true}}$  and  $\mathcal{B}(B^+ \rightarrow \tau^+ \nu_\tau)$ , obtained from (28), setting  $\gamma = 68^\circ$  and choosing two values for  $|V_{ub}|$  corresponding to two scenarios defined in Section 1. We observe that for both choices of  $|V_{ub}|$  the data show significant deviations from the SM predictions but the character of the NP which could cure these tensions depends on the choice of  $|V_{ub}|$  as already discussed in detail in [4] and summarized at the beginning of this paper.

What is striking in this table is that the predicted central values of  $\Delta M_s$  and  $\Delta M_d$ , although slightly above the data, are both in good agreement with the latter when hadronic uncertainties are taken into account. In particular the central value of the ratio  $\Delta M_s/\Delta M_d$  is very close to the data:

$$\left(\frac{\Delta M_s}{\Delta M_d}\right)_{\text{SM}} = 34.5 \pm 3.0 \quad \text{exp : } 35.0 \pm 0.3 \quad (30)$$

$G_F = 1.16637(1) \times 10^{-5} \text{ GeV}^{-2}$ [19]	$m_{B_d} = 5279.5(3) \text{ MeV}$ [19]
$M_W = 80.385(15) \text{ GeV}$ [19]	$m_{B_s} = 5366.3(6) \text{ MeV}$ [19]
$\sin^2 \theta_W = 0.23116(13)$ [19]	$F_{B_d} = (190.6 \pm 4.7) \text{ MeV}$ [21]
$\alpha(M_Z) = 1/127.9$ [19]	$F_{B_s} = (227.7 \pm 5.0) \text{ MeV}$ [21]
$\alpha_s(M_Z) = 0.1184(7)$ [19]	$\hat{B}_{B_d} = 1.26(11)$ [21]
$m_u(2 \text{ GeV}) = (2.1 \pm 0.1) \text{ MeV}$ [21]	$\hat{B}_{B_s} = 1.33(6)$ [21]
$m_d(2 \text{ GeV}) = (4.73 \pm 0.12) \text{ MeV}$ [21]	$\hat{B}_{B_s}/\hat{B}_{B_d} = 1.05(7)$ [21]
$m_s(2 \text{ GeV}) = (93.4 \pm 1.1) \text{ MeV}$ [21]	$F_{B_d} \sqrt{\hat{B}_{B_d}} = 226(15) \text{ MeV}$ [21]
$m_c(m_c) = (1.279 \pm 0.013) \text{ GeV}$ [61]	$F_{B_s} \sqrt{\hat{B}_{B_s}} = 279(15) \text{ MeV}$ [21]
$m_b(m_b) = 4.19_{-0.06}^{+0.18} \text{ GeV}$ [19]	$\xi = 1.237(32)$ [21]
$m_t(m_t) = 163(1) \text{ GeV}$ [21, 62]	$\eta_B = 0.55(1)$ [55, 56]
$M_t = 172.9 \pm 0.6 \pm 0.9 \text{ GeV}$ [19]	$\Delta M_d = 0.507(4) \text{ ps}^{-1}$ [19]
$m_K = 497.614(24) \text{ MeV}$ [19]	$\Delta M_s = 17.73(5) \text{ ps}^{-1}$ [63, 64]
$F_K = 156.1(11) \text{ MeV}$ [21]	$S_{\psi K_S} = 0.679(20)$ [19]
$\hat{B}_K = 0.764(10)$ [21]	$S_{\psi\phi} = 0.0002 \pm 0.087$ [20]
$\kappa_\epsilon = 0.94(2)$ [6, 58]	$\mathcal{B}(B^+ \rightarrow \tau^+ \nu) = (1.64 \pm 0.34) \times 10^{-4}$ [19]
$\eta_1 = 1.87(76)$ [33]	$\tau_{B^\pm} = (1641 \pm 8) \times 10^{-3} \text{ ps}$ [19]
$\eta_2 = 0.5765(65)$ [55]	$ V_{us}  = 0.2252(9)$ [19]
$\eta_3 = 0.496(47)$ [57]	$ V_{cb}  = (40.6 \pm 1.3) \times 10^{-3}$ [19]
$\Delta M_K = 0.5292(9) \times 10^{-2} \text{ ps}^{-1}$ [19]	$ V_{ub}^{\text{incl.}}  = (4.27 \pm 0.38) \times 10^{-3}$ [19]
$ \varepsilon_K  = 2.228(11) \times 10^{-3}$ [19]	$ V_{ub}^{\text{excl.}}  = (3.12 \pm 0.26) \times 10^{-3}$ [21]

Table 1: Values of the experimental and theoretical quantities used as input parameters.

	Scenario 1:	Scenario 2:	Experiment
$ \varepsilon_K $	$1.72(22) \cdot 10^{-3}$	$2.28(28) \cdot 10^{-3}$	$2.228(11) \times 10^{-3}$
$(\sin 2\beta)_{\text{true}}$	0.623(25)	0.812(23)	0.679(20)
$\Delta M_s [\text{ps}^{-1}]$	19.0(21)	19.1(21)	17.73(5)
$\Delta M_d [\text{ps}^{-1}]$	0.55(6)	0.56(6)	0.507(4)
$\mathcal{B}(B^+ \rightarrow \tau^+ \nu_\tau)$	$0.62(14) \cdot 10^{-4}$	$1.19(20) \cdot 10^{-4}$	$0.99(25) \times 10^{-4}$

Table 2: SM prediction for various observables for  $|V_{ub}| = 3.1 \cdot 10^{-3}$  and  $|V_{ub}| = 4.3 \cdot 10^{-3}$  and  $\gamma = 68^\circ$  compared to experiment.

These results depend on the lattice input and in the case of  $\Delta M_d$  on the value of  $\gamma$ . Therefore to get a better insight both lattice input and the tree level determination of  $\gamma$  have to improve.

We also note that in the case of  $B^+ \rightarrow \tau^+ \nu_\tau$  the disagreement of the data with the SM softened significantly with the new result from Belle Collaboration [65]. The new world

average provided by the UFit collaboration of  $\mathcal{B}(B^+ \rightarrow \tau^+ \nu)_{\text{exp}} = (0.99 \pm 0.25) \times 10^{-4}$  [66] given in Table 2 is in perfect agreement with the SM in scenario S2 and only by  $1.5\sigma$  above the SM value in scenario S1.

## 4.2 Results in $MU(2)^3$ Models

Let us begin the discussion with the mass differences  $\Delta M_{s,d}$ . The  $MU(2)^3$  models just passed a very important test. The new parameter free prediction (26) of these models agrees with data. To bring the separate values of  $\Delta M_d$  and  $\Delta M_s$  closer to the data we can just take

$$r_B = 0.93 \pm 0.10. \quad (31)$$

This is clearly possible in these models because NP contributions generating the non-vanishing phase  $\varphi_{\text{new}}$  can interfere destructively with SM contribution. We will see an explicit example in the next Section. Moreover, in contrast to CMFV models this NP effect has no impact on  $\varepsilon_K$ . But it should be noted that while we got this result for free, in a concrete dynamical  $MU(2)^3$  model (31) will constitute a constraint on the fundamental parameters of this model.

We have still two parameters to our disposal,  $r_K$  and  $\varphi_{\text{new}}$ .  $r_K$  enters  $\varepsilon_K$ , while  $\varphi_{\text{new}}$  the CP asymmetries  $S_{\psi K_S}$  and  $S_{\psi\phi}$ . At first sight one could consider these two parameters independently, but one should notice that  $\varepsilon_K$  and  $S_{\psi K_S}$  depend on the same phase  $\beta$ , which in turn depends sensitively on  $|V_{ub}|$  and very mildly on  $\gamma$ . Therefore, in order to get the full picture whether a given model works or not we have to consider  $S_{\psi K_S}$ ,  $S_{\psi\phi}$ ,  $\varepsilon_K$ ,  $|V_{ub}|$  and the two new parameters simultaneously as they are correlated with each other when the experimental data are taken into account.

In Fig. 1 we show  $S_{\psi K_S}$  vs.  $S_{\psi\phi}$  for different values of  $|V_{ub}|$  for  $\gamma = 68^\circ \pm 10^\circ$ . The light gray (dark gray) area shows  $1\sigma$  ( $2\sigma$ ) experimental ranges for both asymmetries. The black dots represent the case of vanishing new phases  $\varphi_{B_q}$ , in which case the formulae in (22) apply. As expected for this case we observe a strong variation of  $S_{\psi K_S}$  with  $|V_{ub}|$  but only tiny  $|V_{ub}|$ -dependence in  $S_{\psi\phi}$ . The SM and CMFV are represented here roughly by a black dot on the cyan  $|V_{ub}| = 3.4 \times 10^{-3}$  line.

We would like to emphasize that the uncertainties in the plot in Fig. 1 for fixed  $|V_{ub}|$  are very small. Indeed this plot is based on the unitarity of the CKM matrix and the  $U(2)^3$  relation between new phases in (1). The very small uncertainty to the value of  $\gamma$  can be understood as follows.  $S_{\psi\phi}$  depends very weakly on  $\gamma$  as it is an order  $\lambda^2$  effect.  $S_{\psi K_S}$  depends also weakly on  $\gamma$  because as seen in the unitarity triangle, the angle  $\beta$  relevant for  $S_{\psi K_S}$  is an orthogonal variable to  $\gamma$ . The remaining theoretical uncertainties due to QCD-penguins are small [34–45] and when both asymmetries will be measured precisely, also these uncertainties are expected to be fully under control.

In Fig. 2 we show  $S_{\psi\phi}$  vs.  $|V_{ub}|$  in  $MU(2)^3$  models for different values of  $S_{\psi K_S}$ . The information in this figure is equivalent to the previous one but it could turn out to be more useful than the latter once  $S_{\psi K_S}$  will be measured very precisely at the LHC.

Figs. 1 and 2 exhibit a number of interesting features that we would like to emphasize now.

- For values in the ballpark of inclusive determinations and close to the central value in (5) we find, in agreement with [8], that  $S_{\psi\phi}$  is positive and larger than the SM value. The same applies to a specific  $U(2)^3$  model,  $2\text{HDM}_{\overline{\text{MFV}}}$  with the dominance of flavour blind phases in the Higgs potential, as found in [4, 46–48]<sup>6</sup>.
- Already now within  $MU(2)^3$  models we find a  $1\sigma$  ( $2\sigma$ ) bound

$$|V_{ub}| \leq 3.7 \times 10^{-3} (4.4 \times 10^{-3}). \quad (32)$$

- An important new result following from Fig. 1 is that, in contrast to  $2\text{HDM}_{\overline{\text{MFV}}}$ , in the  $MU(2)^3$  models *negative* values of  $S_{\psi\phi}$  can be in principle accommodated so that a future measurement of a negative  $S_{\psi\phi}$  would not rule out this class of models. However, such a measurement would favour in this framework  $|V_{ub}|$  in the ballpark of exclusive determinations.
- As seen in particular in Fig. 2 precise measurements of  $S_{\psi K_S}$  vs.  $S_{\psi\phi}$  would allow in this framework a rather precise determination of  $|V_{ub}|$  subject to much smaller hadronic uncertainties than the usual determinations by means of semi-leptonic  $B$  decays. Already the measurements of both asymmetries with errors of  $\pm 0.01$  would allow the determination of  $|V_{ub}|$  with an impressive accuracy of 2%. However, at this order of accuracy the corrections from QCD-penguins to the formulae in (24) should be included.
- On the other hand once  $S_{\psi K_S}$ ,  $S_{\psi\phi}$  and  $|V_{ub}|$  will be determined one day independently of any  $MU(2)^3$  assumptions the plots in Figs. 1 and 2 will allow to test the  $MU(2)^3$  models as a general framework. If this test will be successfully passed, the selection of the concrete successful  $MU(2)^3$  model will require the inclusion of other observables.

In the context of the last point, the  $\varepsilon_K$  constraint should be emphasized. In particular, in the case of a low value of  $|V_{ub}|$ , as seen in Table 2 some enhancement of the function  $S_K$  over its SM value is required. That is  $r_K > 1$  which is very natural in  $MU(2)^3$  models.

In order to illustrate this point quantitatively, we choose the nominal values of the CKM parameters in (27), set the values of other input parameters at their central values in Table 1 and show in Fig. 3  $|\varepsilon_K|$  as a function of  $|V_{ub}|$  for different values of  $r_K$ . To this end we set  $S_{\psi K_S}$  at its central experimental value. As this specifies uniquely the

---

<sup>6</sup>The operators responsible for NP contributions in this case are the  $Q_{1,2}^{\text{SLL}}$  with the  $(S-P) \times (S-P)$  structure but they also imply  $\varphi_{B_d} = \varphi_{B_s}$ . On the other hand in  $2\text{HDM}_{\overline{\text{MFV}}}$   $r_K = 1$  to a good approximation.

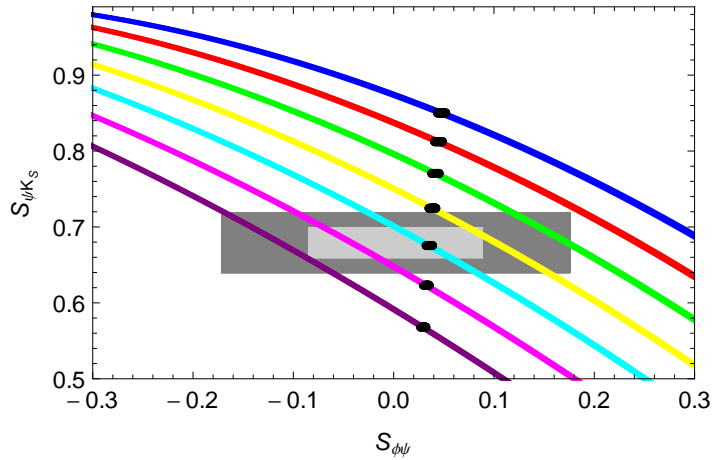


Figure 1:  $S_{\psi K_S}$  vs.  $S_{\psi\phi}$  in models with  $U(2)^3$  symmetry for different values of  $|V_{ub}|$  and  $\gamma \in [58^\circ, 78^\circ]$ . From top to bottom:  $|V_{ub}| = 0.0046$  (blue), 0.0043 (red), 0.0040 (green), 0.0037 (yellow), 0.0034 (cyan), 0.0031 (magenta), 0.0028 (purple). Light/dark gray: experimental  $1\sigma/2\sigma$  region.

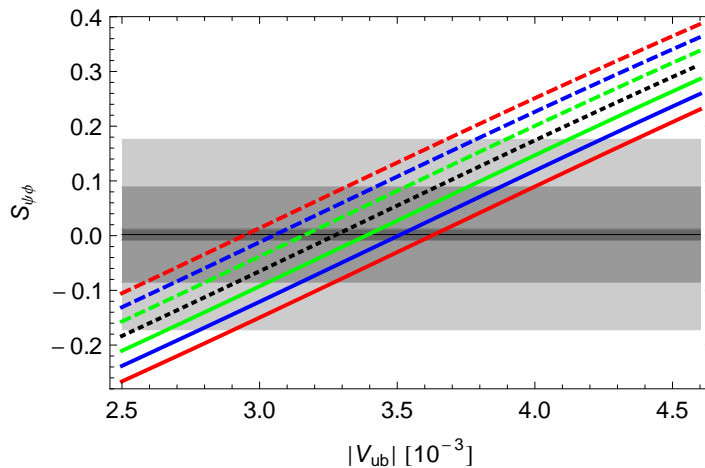


Figure 2:  $S_{\psi\phi}$  vs.  $|V_{ub}|$  in models with  $U(2)^3$  symmetry for different values of  $S_{\psi K_S}$  (experimental central value and 1, 2 and 3 $\sigma$  values). From top to bottom:  $S_{\psi K_S} = 0.619$  (red dashed), 0.639 (blue dashed), 0.659 (green dashed), 0.679 (black dotted), 0.699 (green solid), 0.719 (blue solid), 0.739 (red solid). Horizontal black line: experimental central value  $S_{\psi\phi}^{exp} = 0.002$ , dark gray region:  $0.002 \pm 0.01$ , middle gray: experimental  $1\sigma$  range, light gray: experimental  $2\sigma$  range.

correlation between  $S_{\psi\phi}$  and  $|V_{ub}|$ , we also show in Fig. 4  $|\varepsilon_K|$  as a function of  $S_{\psi\phi}$ . The latter correlation is interesting in itself as it shows that in a given specific  $MU(2)^3$  model also correlations between  $B$ -physics and  $K$ -physics are possible.

At this point we should emphasize the difference in the quality of the correlations in

Figs. 1 and 2 on one hand and in Figs. 3 and 4 on the other hand. While for a fixed value of  $|V_{ub}|$  the theoretical uncertainties in Figs. 1 and 2 are very small, this is certainly not the case of Figs. 3 and 4 in which  $|\varepsilon_K|$  is involved. Indeed, as seen in Table 2 the error in the SM prediction for  $|\varepsilon_K|$  amounts to roughly  $\pm 12\%$ . As this error originates dominantly from  $|V_{cb}|$ ,  $\eta_1$  and  $\hat{B}_K$ , it is practically independent of  $|V_{ub}|$ . Therefore, in reality the values of  $r_K$  extracted for fixed values of  $|V_{ub}|$  from these plots have an error of roughly  $\pm 12\%$ , which makes the tests of these correlations difficult at present. We show this uncertainty in Figs. 3 and 4 by incorporating it in the experimental value of  $|\varepsilon_K|$ .

Bearing this problem in mind in the case of a negative  $S_{\psi\phi}$  chosen by nature and consequently small  $|V_{ub}|$  implied by  $U(2)^3$  symmetry, an enhancement of  $|\varepsilon_K|$  by roughly 20% is required.

The latter condition is not satisfied in the  $2\text{HDM}_{\overline{\text{MFV}}}$  model which in the limit of the dominance of flavour blind phases in the Higgs potential exhibits  $U(2)^3$  symmetry. As in this model NP contributions to  $\varepsilon_K$  are negligible, this model favours  $|V_{ub}| \geq 3.6 \cdot 10^{-3}$  [4, 48] and this implies  $S_{\psi\phi} \geq 0.05$ . Finding in the future that nature chooses a *negative* value of  $S_{\psi\phi}$  and/or small (exclusive) value of  $|V_{ub}|$  would put  $2\text{HDM}_{\overline{\text{MFV}}}$  into difficulties. Clear cut conclusion can only be reached when theoretical error on  $\varepsilon_K$  will be decreased.

Also a decrease of the experimental error on  $S_{\psi\phi}$  without the change of its central value would be problematic for this model.

On the other hand as we have seen  $MU(2)^3$  models can be in principle consistent with a negative value of  $S_{\psi\phi}$  provided

$$|V_{ub}| \leq 3.3 \times 10^{-3}, \quad S_K \geq 1.20 S_0(x_t), \quad (33)$$

with precise values depending on  $S_{\psi K_S}$  as seen in Fig. 2 and uncertainties in  $\varepsilon_K$  discussed above.

However, as is well known, the branching ratio for  $B^+ \rightarrow \tau^+ \nu_\tau$  depends sensitively on  $|V_{ub}|$  and this may not allow negative values of  $S_{\psi\phi}$ . As in  $U(2)^3$  models there is no obvious possibility to enhance the branching ratio in question, we use the SM expression for it and show in Fig. 5 for fixed  $S_{\psi K_S}$  the correlation between  $\mathcal{B}(B^+ \rightarrow \tau^+ \nu_\tau)$  and  $S_{\psi\phi}$  for different values of  $F_{B^+}$ . We show there also the present world average for  $\mathcal{B}(B^+ \rightarrow \tau^+ \nu_\tau)$ . Evidently we have to wait for improved data on the quantities involved but a *negative*  $S_{\psi\phi}$  in this framework has a clear tendency to imply values of  $\mathcal{B}(B^+ \rightarrow \tau^+ \nu_\tau)$  below the present data.

In this context we would also like to remark that in CMFV the increase of  $F_{B^+}$  while improving the agreement for  $\mathcal{B}(B^+ \rightarrow \tau^+ \nu_\tau)$  would worsen the agreement of the theory and data for  $\Delta M_{s,d}$ . In the  $MU(2)^3$  models this change could in principle be compensated by non-MFV effects in  $\Delta M_{s,d}$ .

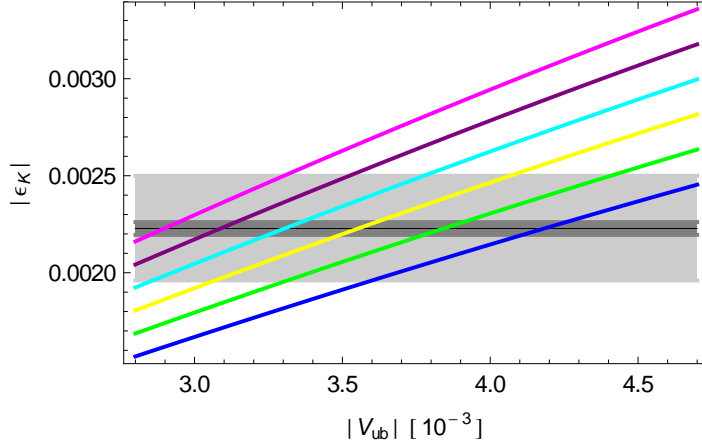


Figure 3:  $|\varepsilon_K|$  vs.  $|V_{ub}|$  in models with  $U(2)^3$  symmetry for fixed  $S_{\psi_{K_S}} = 0.679$  and different values of the enhancement factor  $r_K$ . From top to bottom:  $r_K = 1.5$  (magenta), 1.4 (purple), 1.3 (cyan), 1.2 (yellow), 1.1 (green), 1 (blue, SM prediction)). Dark gray region: experimental  $3\sigma$  range of  $|\varepsilon_K|$ . Light gray region: theoretical uncertainty in  $|\varepsilon_K|$ .

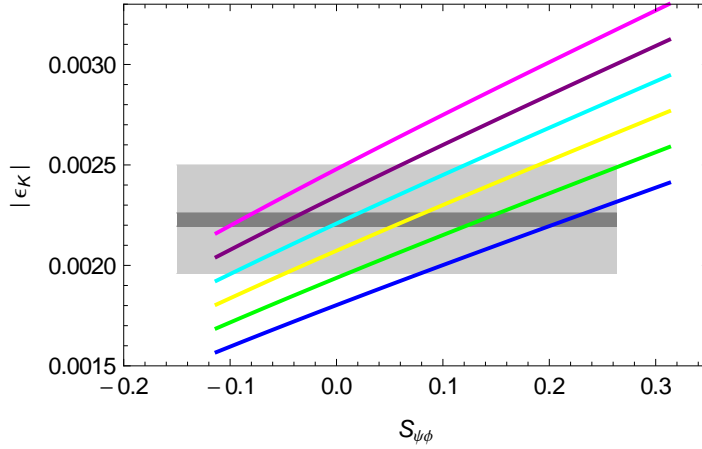


Figure 4:  $|\varepsilon_K|$  vs.  $S_{\psi\phi}$  in models with  $U(2)^3$  symmetry for fixed  $S_{\psi_{K_S}} = 0.679$ ,  $|V_{ub}| \in [0.0028, 0.0046]$  and different values of the enhancement factor  $r_K$  (colours for  $r_K$  as in Fig. 3).

## 5 Strategy for Testing $MU(2)^3$ Scenario

### 5.1 Preliminaries

In order to test any NP scenario through flavour physics we need a good precision on the CKM parameters from tree-level decays and on the non-perturbative parameters entering  $\Delta F = 2$  observables. Concerning the latter, the absence of contributions

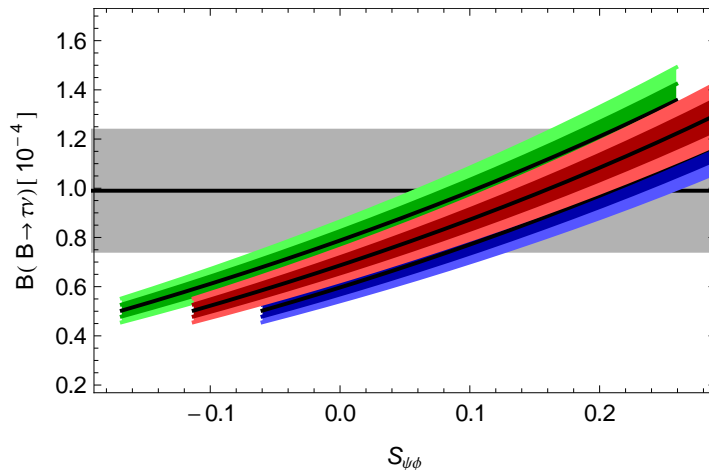


Figure 5:  $\mathcal{B}(B^+ \rightarrow \tau^+ \nu_\tau)$  vs.  $S_{\psi\phi}$  in models with  $U(2)^3$  symmetry for  $S_{\psi K_S} = 0.679$  (experimental central value, red), 0.719 (upper  $2\sigma$  value, green) and 0.639 (lower  $2\sigma$  value, blue) and  $|V_{ub}| \in [0.0028, 0.0046]$  and different values of  $F_{B^+} = 190.6$  MeV (central value, black),  $(190.6 \pm 4.6)$  MeV ( $1\sigma$  region, dark coloured region),  $(190.6 \pm 9.2)$  MeV ( $2\sigma$  region, light coloured region). We show  $1\sigma$  experimental range for  $\mathcal{B}(B^+ \rightarrow \tau^+ \nu_\tau)$  (gray).

from new operators does not increase the hadronic uncertainties in the  $MU(2)^3$  models in question relatively to SM and CMFV models. Moreover, lattice calculations made significant progress in the last years [21, 67–69] and further progress is expected in the coming years.

The optimal choice for the input parameters beyond those listed in (27) would certainly be  $|V_{ub}|$  determined in tree-level decays without any or only small pollution from NP. However, as we have seen the present status of  $|V_{ub}|$  is very unsatisfactory and it is likely that only after Super-Belle and later Super-B will provide the data and improved theory we will know a significantly more precise value of  $|V_{ub}|$ .

However, as pointed out in [70], a very efficient method to determine the CKM parameters is to use in addition to the set (27), the asymmetry  $S_{\psi K_S}$ . That is the use of the set  $(\gamma, \beta)$  allows with a smaller precision on both variables to determine the apex of the Unitarity Triangle  $(\bar{\rho}, \bar{\eta})$  than it is required if for instance  $(\beta, R_t)$  or in particular  $(\gamma, R_t)$  are used. Now  $S_{\psi K_S}$  is polluted by NP but in the  $MU(2)^3$  scenario this pollution has a very simple structure represented by a universal new phase  $\varphi_{\text{new}}$ . Moreover this phase can be determined by invoking precisely  $S_{\psi\phi}$ .

Thus we are led to a new strategy for the determination of CKM parameters which generally would not be evidently efficient but in this simple NP scenario could indeed turn out to be useful in the second phase of the LHC. Of course, we are aware of possible QCD penguin effects absent in our analysis, that one has to consider in order to reach sufficient precision on the extraction of the parameters involved from the data on  $S_{\psi K_S}$

and  $S_{\psi\phi}$ . However, this issue is a science for itself [34–45] and clearly beyond the scope of our paper. Our strategy then involves five steps.

## 5.2 Strategy in Five Steps

### Step 1.

Use the following experimental input from tree diagram dominated decays

$$|V_{us}|, \quad |V_{cb}|, \quad \gamma, \quad S_{\psi K_S}, \quad S_{\psi\phi}. \quad (34)$$

$|V_{us}|$  is already precisely known and the accuracy on  $\gamma$  should be improved in the coming years by the LHCb.  $|V_{cb}|$  is known presently with an accuracy of 2 – 3% and improvements are expected from SuperKEKB and SuperB.

### Step 2.

Using the formulae of Section 3 together with (28) and (29) find

$$|V_{ub}|, \quad \varphi_{\text{new}}, \quad \beta = \beta_{\text{true}}. \quad (35)$$

### Step 3.

Using future improved values of non-perturbative parameters from lattice calculations extract

$$r_K, \quad r_B. \quad (36)$$

If  $r_K$  turns out to be below unity, this NP scenario will be put into difficulties, but presently the data favour  $r_K$  above one.

### Step 4.

Extract  $|V_{ub}|$  from future data and improved theory and compare the result with the value implied by Fig. 1. This is a crucial test of this NP scenario. Assuming that this test is passed go to a specific model in the last step.

### Step 5.

Verify whether a given  $MU(2)^3$  model is consistent with the extracted values of

$$r_K, \quad r_B, \quad \varphi_{\text{new}}. \quad (37)$$

We will now illustrate this strategy with a specific example.

### 5.3 Explicit Example

The specific supersymmetric model studied in [8,9] has precisely the structure of  $MU(2)^3$  and with respect to  $\Delta F = 2$  transitions can be summarized simply as follows:

$$r_K = 1 + |\xi_L|^4 F_0, \quad (38)$$

$$r_B e^{2i\varphi_{\text{new}}} = 1 + \xi_L^2 F_0, \quad (39)$$

where

$$\xi_L = \frac{s_L c_d}{|V_{ts}|} e^{i\gamma_L}, \quad (40)$$

with  $\gamma_L$  being an arbitrary phase and  $s_L$  and  $c_d$  defined in [8,9]. Next

$$F_0 = \frac{2}{3} \left( \frac{g_s}{g} \right)^4 \frac{M_W^3}{m_{Q_3}^2 S_0(x_t)} \frac{1}{S_0(x_t)} \left[ f_0(x_g) + \mathcal{O} \left( \frac{m_{Q_t}^2}{m_{Q_h}^2} \right) \right], \quad (41)$$

$$f_0(x) = \frac{11 + 8x - 19x^2 + 26x \log x + 4x^2 \log x}{3(1-x)^3}, \quad (42)$$

$$x_g = \frac{m_{\tilde{g}}^2}{m_{Q_3}^2}, \quad f_0(1) = 1. \quad (43)$$

Here  $m_{\tilde{g}}$  is the gluino mass and  $m_{Q_3}^2$  the third generation squark mass. Indeed, this model has three new free parameters

$$|\xi_L|, \quad F_0, \quad \gamma_L. \quad (44)$$

In [8] in Fig. 2 it is shown that for  $400 \text{ GeV} \lesssim m_{\tilde{g}} \lesssim 1000 \text{ GeV}$  and  $500 \text{ GeV} \lesssim m_{Q_3} \lesssim 1200 \text{ GeV}$  one gets  $F_0$  roughly between 0.1 and 0.02 and  $|\xi_L|$  is of  $\mathcal{O}(1)$ .

We follow the steps from the previous section. As inputs we fix  $|V_{us}| = 0.2252$ ,  $|V_{cb}| = 0.0406$  and  $\gamma = 68^\circ$  and use three different values for  $S_{\psi K_S}$  corresponding to its experimental  $1\sigma$  range (0.659, 0.679, 0.699) and for  $S_{\psi\phi}$  we use  $-0.2$ ,  $-0.1$ ,  $0$ ,  $0.1$  and  $0.2$ . This is listed in the first two columns of Table 3. As already visualized in Fig. 1 and 2 with this information we can determine  $|V_{ub}|$  and also  $2\varphi_{\text{new}}$  and  $\beta_{\text{true}}$ . The results are written in columns 3–5 in Table 3. As a next step we want to shift  $|\varepsilon_K|$  to its measured value  $2.228 \cdot 10^{-3}$  allowing for a 12% error on  $r_K$  to account for the uncertainties in  $|\varepsilon_K|$ . This leads to the values of  $r_K$  quoted in Tab. 3. Although there is no direct correlation between  $K$  and  $B_{d,s}$  sector in  $U(2)^3$  models we get a connection due to the dependence of  $|\varepsilon_K|$  on  $\beta_{\text{true}} = \beta_{\text{true}}(|V_{ub}|)$ . Fixing  $r_B$  in our explicit example we get a one-to-one relation between  $|\xi_L|^2 F_0$  and  $2\gamma_L$  and between  $|\xi_L|^2 F_0$  and  $2\varphi_{\text{new}}$  and thus also between  $2\gamma_L$  and  $2\varphi_{\text{new}}$ . This is shown for  $r_B = 0.93$ ,  $r_B = 1$  and  $r_B = 1.1$  in Fig. 6. In the following we set  $r_B = 0.93$  as suggested by current lattice values and calculate the corresponding model parameter  $|\xi_L|^2 F_0$  using Eq. (39). Using this and  $r_K$

we can derive a range for  $|\xi_L|^2$  and then also for  $F_0$  (see last three columns of Table 3). But  $|\xi_L|^2$  and  $F_0$  have to be combined such that one gets the right  $|\xi_L|^2 F_0$  from the 7th column (e.g. the lower bound from  $|\xi_L|^2$  and the upper bound from  $F_0$ ). The derived values of  $F_0$  can now be compared with the range 0.02–0.10 that is obtained for reasonable gluino and sbottom masses. For  $F_0 \leq 0.02$  one needs rather heavy gluino and sbottom masses. For  $S_{\psi\phi} = 0.2$  where  $|V_{ub}|$  is near the inclusive value one needs very light gluino and sbottom masses near 300 GeV. The limiting factor for  $S_{\psi\phi} = -0.2$  in this model are not the SUSY masses but the small value of  $|V_{ub}| \approx 0.0024$ . However  $S_{\psi\phi} = -0.1$  could still be reached for reasonable gluino and sbottom masses in case of  $|V_{ub}| \approx 0.0028$ .

$S_{\psi K_S}$	$S_{\psi\phi}$	$ V_{ub} $	$2\varphi_{\text{new}}$	$\beta_{\text{true}}$	$r_K$	$ \xi_L ^2 F_0$	$ \xi_L ^2$	$F_0$
0.679	0.2	0.0041	-9.1°	25.9°	$1.02 \pm 0.12$	0.169	[0,0.83]	$\geq 0.204$
0.679	0.1	0.0037	-3.5°	23.2°	$1.15 \pm 0.14$	0.092	[0.11,3.17]	[0.029,0.838]
0.679	0	0.0033	2.0°	20.4°	$1.31 \pm 0.16$	0.078	[1.93,6.05]	[0.013,0.040]
0.679	-0.1	0.0028	7.5°	17.7°	$1.52 \pm 0.18$	0.145	[2.35,4.83]	[0.030,0.062]
0.679	-0.2	0.0024	13.0°	14.9°	$1.81 \pm 0.22$	0.233	[2.53,4.42]	[0.053,0.092]
0.659	0.2	0.0040	-9.1°	25.2°	$1.05 \pm 0.13$	0.169	[0,1.06]	$\geq 0.159$
0.659	0.1	0.0036	-3.6°	22.4°	$1.19 \pm 0.14$	0.093	[0.54,3.56]	[0.026,0.172]
0.659	0	0.0032	1.9°	19.7°	$1.36 \pm 0.16$	0.077	[2.60,6.76]	[0.011,0.030]
0.659	-0.1	0.0027	7.4°	16.9°	$1.59 \pm 0.19$	0.143	[2.79,5.44]	[0.026,0.051]
0.659	-0.2	0.0023	12.9°	14.1°	$1.90 \pm 0.23$	0.231	[2.90,4.89]	[0.047,0.080]
0.699	0.2	0.0042	-9.0°	26.7°	$0.99 \pm 0.12$	0.168	[0,0.66]	$\geq 0.256$
0.699	0.1	0.0038	-3.5°	23.9°	$1.11 \pm 0.13$	0.092	[0,2.62]	$\geq 0.035$
0.699	0	0.0034	2.0°	21.2°	$1.26 \pm 0.15$	0.078	[1.42,5.28]	[0.015,0.055]
0.699	-0.1	0.0030	7.5°	18.4°	$1.46 \pm 0.18$	0.145	[1.93,4.42]	[0.033,0.075]
0.699	-0.2	0.0025	13.1°	15.6°	$1.72 \pm 0.21$	0.235	[2.17,3.96]	[0.059,0.108]

Table 3: *Explicit  $MU(2)^3$  SUSY example. Column 1–5 correspond to step 1 and 2 where for different inputs of  $S_{\psi K_S}$  and  $S_{\psi\phi}$  we determine the corresponding  $|V_{ub}|$ ,  $2\varphi_{\text{new}}$  and  $\beta_{\text{true}}$ .  $r_K$  is derived such that  $|\varepsilon_K| = 2.228 \cdot 10^{-3}$  with a 12% error on  $r_K$ . The corresponding model parameters are listed in column 7–9 using  $r_B = 0.93$ . For more details see text.*

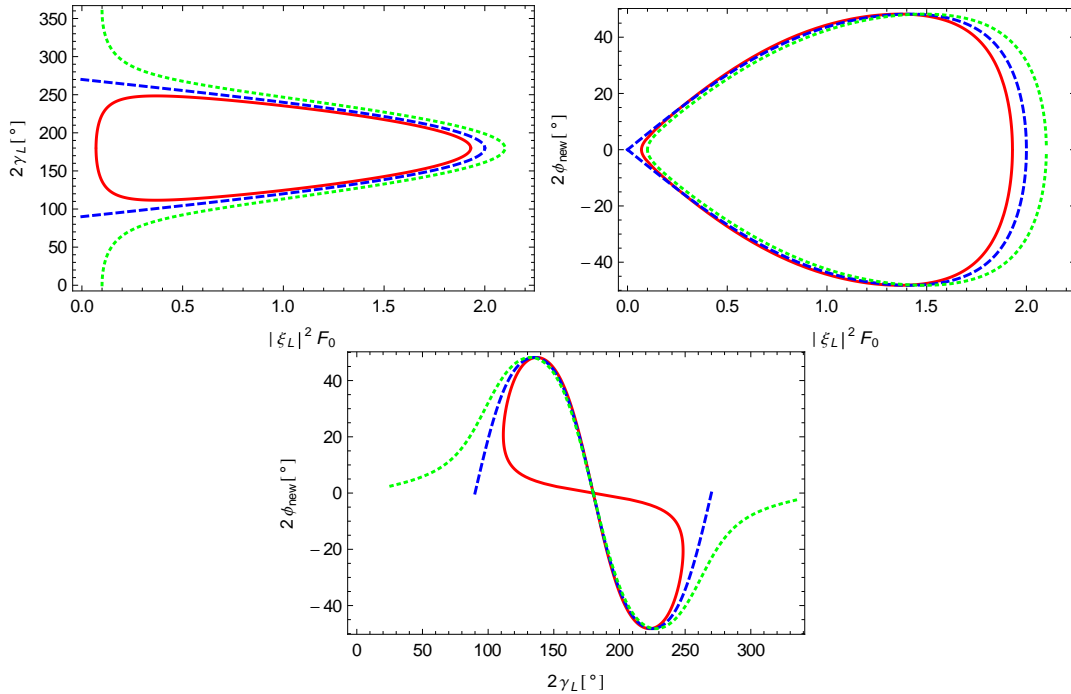


Figure 6: For fixed  $r_B = 0.93$  (red solid),  $r_B = 1$  (blue dashed) and  $r_B = 1.1$  (green dotted) relation between  $2\gamma_L$ ,  $2\phi_{new}$  and  $|\xi_L|^2 F_0$ .

## 6 Rare Decays

### 6.1 Preliminaries

Here we just want to describe briefly the pattern of flavour violation in  $MU(2)^3$  models in rare  $B$  and  $K$  decays and compare it to the one in CMFV models.

First we would like to emphasize that the flavour physics in the  $MU(2)^3$  models can be parametrized, similar to the LHT model, by a set of master functions  $F_i$  ( $i = K, d, s$ ):

$$S_i \equiv |S_i| e^{i\theta_s^i}, \quad X_i \equiv |X_i| e^{i\theta_X^i}, \quad Y_i \equiv |Y_i| e^{i\theta_Y^i}, \quad Z_i \equiv |Z_i| e^{i\theta_Z^i}, \quad (45)$$

$$E_i \equiv |E_i| e^{i\theta_E^i}, \quad D'_i \equiv |D'_i| e^{i\theta_{D'}^i}, \quad E'_i \equiv |E'_i| e^{i\theta_{E'}^i}, \quad (46)$$

with the following properties implied by  $U(2)^3$  symmetry:

$$|F_d| = |F_s|, \quad \theta_F^K = 0, \quad \theta_F^d = \theta_F^s \equiv \theta_F \quad (47)$$

that allow to distinguish these models not only from CMFV models but also models with non-MFV sources like LHT and Randall-Sundrum models. The information which function enters which decay can be found in [2].

On the other hand as discussed in [9], contrary to  $\Delta F = 2$  transitions, where the pattern of deviations from the SM is unambiguously dictated by  $U(2)^3$  symmetry, the predictions for  $\Delta F = 1$  processes are more model dependent. In particular, while the quark transitions, similarly to MFV, are governed by the CKM matrix and left-handed currents, the lepton currents in FCNC processes could in addition to left-handed currents have right-handed component absent in the SM and CMFV. Yet, independently of these new operators the universality of NP contributions to  $B_d$  and  $B_s$  decays implied by the  $U(2)^3$  symmetry is intact and in what follows we will only discuss its consequences below.

## 6.2 Rare $B$ Decays

In view of the universality of NP contributions to  $B_d$  and  $B_s$  decays in question, several CMFV relations involving only  $B_{d,s}$  observables are not modified. In particular,

$$\frac{\mathcal{B}(B \rightarrow X_d \nu \bar{\nu})}{\mathcal{B}(B \rightarrow X_s \nu \bar{\nu})} = \left| \frac{V_{td}}{V_{ts}} \right|^2 \quad (48)$$

$$\frac{\mathcal{B}(B_d \rightarrow \mu^+ \mu^-)}{\mathcal{B}(B_s \rightarrow \mu^+ \mu^-)} = \frac{\tau(B_d) m_{B_d} F_{B_d}^2}{\tau(B_s) m_{B_s} F_{B_s}^2} \left| \frac{V_{td}}{V_{ts}} \right|^2 \quad (49)$$

remain valid. Moreover, combining (26) and (49) one obtains [71]

$$\frac{\mathcal{B}(B_s \rightarrow \mu^+ \mu^-)}{\mathcal{B}(B_d \rightarrow \mu^+ \mu^-)} = \frac{\hat{B}_{B_d} \tau(B_s) \Delta M_s}{\hat{B}_{B_s} \tau(B_d) \Delta M_d}, \quad (50)$$

that does not involve  $F_{B_q}$  and CKM parameters and consequently contains smaller hadronic and parametric uncertainties than the formulae considered above. It involves only measurable quantities except for the ratio  $\hat{B}_s/\hat{B}_d$  that is already now known from lattice calculations with respectable precision [21, 72] and this precision will be improved in the coming years.

The formulae in (49) imply that

$$\left( \frac{\mathcal{B}(B_s \rightarrow \mu^+ \mu^-)}{\mathcal{B}(B_d \rightarrow \mu^+ \mu^-)} \right)_{\text{MU}(2)^3} = \left( \frac{\mathcal{B}(B_s \rightarrow \mu^+ \mu^-)}{\mathcal{B}(B_d \rightarrow \mu^+ \mu^-)} \right)_{\text{SM}}. \quad (51)$$

Now, the most recent data from LHCb tell us that the nature does not allow for large enhancements of these branching ratios. Indeed the most recent upper bounds from LHCb, ATLAS and CMS at 95% C.L. read [73, 74]

$$\mathcal{B}(B_s \rightarrow \mu^+ \mu^-) = (3.2_{-1.2}^{+1.5}) \times 10^{-9}, \quad \mathcal{B}(B_s \rightarrow \mu^+ \mu^-)^{\text{SM}} = (3.23 \pm 0.27) \times 10^{-9}, \quad (52)$$

$$\mathcal{B}(B_d \rightarrow \mu^+ \mu^-) \leq 9.4 \times 10^{-10}, \quad \mathcal{B}(B_d \rightarrow \mu^+ \mu^-)^{\text{SM}} = (1.07 \pm 0.10) \times 10^{-10}. \quad (53)$$

We have shown also SM predictions for these observables [75]. The corrections from  $\Delta\Gamma_s$ , pointed out in [49,50], are not taken into account in these values. We will comment on them below.

The distinction between CMFV and  $MU(2)^3$  models on the basis of  $\Delta B = 1$  decays can only be made through  $B$  observables in which the universal phase  $\varphi_{\text{new}}$  matters. These are for instance CP-asymmetries in  $B \rightarrow X_{s,d}\gamma$ ,  $B \rightarrow K^*(\varrho)\gamma$  and certain angular observables in  $B \rightarrow K^*\ell^+\ell^-$ . Such an analysis in a supersymmetric framework with  $U(2)^3$  symmetry has been presented in [9].

Here we would like to point out that the decays  $B_{s,d} \rightarrow \mu^+\mu^-$  offer an additional test of the  $MU(2)^3$  models related to CP violation. Indeed, as pointed out in [49, 50] it is possible to define CP-asymmetries  $S_{\mu^+\mu^-}^{s,d}$  [50] analogous to  $S_{\psi K_S}$  and  $S_{\psi\phi}$  that measure the phases of the functions  $Y_{s,d}$  in (45).

The authors of [50] provide a general expression for  $S_{\mu^+\mu^-}^{s,d}$  as functions of Wilson coefficients involved. Using this formula we find that in the  $MU(2)^3$  models these asymmetries are simply given as follows

$$S_{\mu^+\mu^-}^s = S_{\mu^+\mu^-}^d = \sin(2\theta_Y - 2\varphi_{\text{new}}). \quad (54)$$

This simplicity reflects the fact that scalar operators are absent in the models in question. In the SM and CMFV models these asymmetries vanish. As  $S_{\mu^+\mu^-}^{s,d}$  are theoretically clean they should offer a good test of  $MU(2)^3$  models and of any model with new CP-violating phases. Finally, we should remark that the correction factor to the branching ratio  $\mathcal{B}(B_s \rightarrow \mu^+\mu^-)$  of 9% calculated in [50] applies not only to the SM but also to all CMFV models. In  $MU(2)^3$  models it is modified for  $\theta_Y \neq 0$  and this modification is governed by  $\cos(2\theta_Y - 2\varphi_{\text{new}})$ . Thus only in the case of a large  $S_{\mu^+\mu^-}^s$  it will differ visibly from the SM estimate.

When the corrections from  $\Delta\Gamma_s$ , pointed out in [49, 50], are taken into account and removed from the data the experimental result in (52) is reduced by 9% and we find

$$\mathcal{B}(B_s \rightarrow \mu^+\mu^-)_{\text{corr}} = (2.9_{-1.1}^{+1.4}) \times 10^{-9}, \quad (55)$$

that should be compared with the SM result in (52). While the central theoretical value agrees very well with experiment, the large experimental error still allows for NP contributions.

The result in (55) combined with the relation (50) allows now to predict  $\mathcal{B}(B_d \rightarrow \mu^+\mu^-)$  within CMFV and  $MU(2)^3$  models. Using the experimental values for  $\Delta M_{s,d}$  and  $\tau(B_q)$  and the lattice values for  $\hat{B}_{B_q}$  in Table 1 we find

$$\mathcal{B}(B_d \rightarrow \mu^+\mu^-) = (1.0_{-0.3}^{+0.5}) \times 10^{-10}, \quad (\text{CMFV, } MU(2)^3), \quad (56)$$

implying that this result can only be tested after the upgrade of the LHCb experiment.

### 6.3 Rare $K$ Decays

Here to a large extent the pattern of flavour violation is the same as in CMFV models. In particular, the correlations between the following observables and decays

$$\varepsilon_K, \quad K^+ \rightarrow \pi^+ \nu \bar{\nu}, \quad K_L \rightarrow \pi^0 \nu \bar{\nu}, \quad \varepsilon'/\varepsilon \quad (57)$$

is the same as in CMFV models. For non-leptonic transitions this follows from the left-handed structure of flavour violating quark currents. For channels with neutrinos in the final states we expect that only left-handed couplings are relevant. On the other hand in  $K_L \rightarrow \mu^+ \mu^-$  and  $K_L \rightarrow \pi^0 \ell^+ \ell^-$  right-handed currents in the leptonic sector could enter but this depends on the lepton part of a given model. Finally, as the  $MU(2)^3$  symmetry does not imply any correlations between rare  $K$  and  $B$  decays, NP effects in rare  $K$  decays are generally not constrained by rare  $B_{s,d}$  decays, although in specific  $MU(2)^3$  models this could be the case. In this context one should recall stringent correlations between  $K \rightarrow \pi \nu \bar{\nu}$  and  $B \rightarrow X_{s,d} \nu \bar{\nu}$  as well as  $B \rightarrow K^*(K) \nu \bar{\nu}$  decays in CMFV models. These correlations are generally absent here.

## 7 Summary and Conclusions

In the present paper we have analyzed correlations between flavour observables implied by a global  $U(2)^3$  symmetry concentrating on  $MU(2)^3$  models that are analogous to CMFV models. Indeed, while CMFV models are the simplest models with MFV, the  $MU(2)^3$  models are probably the simplest models with non-MFV interactions. As the simple, but non-trivial, structure of these correlations has been already summarized systematically in previous sections we emphasize here only the most important findings.

- A global  $U(2)^3$  symmetry implies a stringent correlation between  $S_{\psi K_S}$ ,  $S_{\psi\phi}$  and  $|V_{ub}|$  that is displayed for  $\gamma = 68^\circ \pm 10^\circ$  in Fig. 1. This correlation constitutes an important test of this NP scenario but to our knowledge has not been discussed so far in the literature.
- $|V_{ub}|$  can be determined by means of future precise measurements of  $S_{\psi K_S}$  and  $S_{\psi\phi}$  that are subject to significantly smaller uncertainties than contained in present determinations of  $|V_{ub}|$  by means of semileptonic B decays. As  $S_{\psi K_S}$  is presently best known among these three observables we have shown in Fig. 2 the correlation between  $S_{\psi\phi}$  and  $|V_{ub}|$ . This correlation demonstrates clearly that *negative* values of  $S_{\psi\phi}$  can be accommodated in this framework provided  $|V_{ub}|$  is sufficiently low.
- A low value of  $|V_{ub}|$  implies that in the SM,  $|\varepsilon_K|$  is significantly below the data. Therefore a given  $MU(2)^3$  model with negative or very small  $S_{\psi\phi}$  must have significant enhancement of  $|\varepsilon_K|$  relative to the SM in order to agree with data. This we have shown in Figs. 3 and 4. Unfortunately, as seen there, the existing

theoretical and parametric uncertainties in the SM evaluation of  $|\varepsilon_K|$  do not allow a precise determination of the necessary enhancement factor  $r_K$  at present.

- The correlation between  $\mathcal{B}(B^+ \rightarrow \tau^+ \nu_\tau)$  and  $S_{\psi\phi}$  given in Fig. 5 will in due time constitute another important constraint on  $MU(2)^3$  models implying that future experimental *negative* values of  $S_{\psi\phi}$  would in this framework predict  $\mathcal{B}(B^+ \rightarrow \tau^+ \nu_\tau) \leq 0.8 \times 10^{-4}$ .
- We have proposed a five step procedure for the determination of free parameters in  $MU(2)^3$  that should be useful before  $|V_{ub}|$  will be better known. We have illustrated this procedure by means of a specific supersymmetric  $MU(2)^3$  model [8].
- In the case of CP-conserving observables several CMFV relations between observables involving only  $B_d$  and  $B_s$  decays are the same as in the SM and CMFV models. In the case of  $K$  decays this is the case for both CP-violating and CP-conserving observables. Therefore an important distinction between CMFV models and  $MU(2)^3$  models will also be offered by looking at CMFV relations between  $K$  and  $B_{s,d}$  flavour observables that are generally violated in  $MU(2)^3$  models.
- Finally we pointed out that  $B_{s,d} \rightarrow \mu^+ \mu^-$  allow to test new CP-violating phases in  $MU(2)^3$  models with the help of CP-asymmetries  $S_{\mu^+\mu^-}^{s,d}$  proposed in [49, 50]. The formula for  $S_{\mu^+\mu^-}^{s,d}$  in  $MU(2)^3$  models turns out to be very simple and is given in (54).

We are looking forward to improved experimental data and improved lattice calculations. The correlations identified in this paper will allow to monitor how the attractive and simple  $MU(2)^3$  models face the future precision flavour data.

### Acknowledgements

We would like to thank Gino Isidori for discussions. This research was done and financed in the context of the ERC Advanced Grant project “FLAVOUR” (267104). AJB would like to thank the organizers of the “Origin of Mass 2012” in Nordita Stockholm for their hospitality which was very helpful in completing the final steps of this work.

## References

- [1] A. J. Buras, P. Gambino, M. Gorbahn, S. Jager, and L. Silvestrini, *Universal unitarity triangle and physics beyond the standard model*, *Phys. Lett.* **B500** (2001) 161–167, [[hep-ph/0007085](#)].
- [2] A. J. Buras, *Minimal flavor violation*, *Acta Phys. Polon.* **B34** (2003) 5615–5668, [[hep-ph/0310208](#)].

- 
- [3] M. Blanke, A. J. Buras, D. Guadagnoli, and C. Tarantino, *Minimal Flavour Violation Waiting for Precise Measurements of  $\Delta M_s$ ,  $S_{\psi\phi}$ ,  $A_{SL}^s$ ,  $|V_{ub}|$ ,  $\gamma$  and  $B_{s,d}^0 \rightarrow \mu^+\mu^-$* , *JHEP* **10** (2006) 003, [[hep-ph/0604057](#)].
- [4] A. J. Buras and J. Girrbach, *BSM models facing the recent LHCb data: A First look*, *Acta Phys.Polon.* **B43** (2012) 1427, [[arXiv:1204.5064](#)].
- [5] E. Lunghi and A. Soni, *Possible Indications of New Physics in  $B_d$ -mixing and in  $\sin(2\beta)$  Determinations*, *Phys. Lett.* **B666** (2008) 162–165, [[arXiv:0803.4340](#)].
- [6] A. J. Buras and D. Guadagnoli, *Correlations among new CP violating effects in  $\Delta F = 2$  observables*, *Phys. Rev.* **D78** (2008) 033005, [[arXiv:0805.3887](#)].
- [7] G. D’Ambrosio, G. F. Giudice, G. Isidori, and A. Strumia, *Minimal flavour violation: An effective field theory approach*, *Nucl. Phys.* **B645** (2002) 155–187, [[hep-ph/0207036](#)].
- [8] R. Barbieri, G. Isidori, J. Jones-Perez, P. Lodone, and D. M. Straub,  *$U(2)$  and Minimal Flavour Violation in Supersymmetry*, *Eur.Phys.J.* **C71** (2011) 1725, [[arXiv:1105.2296](#)].
- [9] R. Barbieri, P. Campli, G. Isidori, F. Sala, and D. M. Straub,  *$B$ -decay CP-asymmetries in SUSY with a  $U(2)^3$  flavour symmetry*, *Eur.Phys.J.* **C71** (2011) 1812, [[arXiv:1108.5125](#)].
- [10] R. Barbieri, D. Buttazzo, F. Sala, and D. M. Straub, *Flavour physics from an approximate  $U(2)^3$  symmetry*, *JHEP* **1207** (2012) 181, [[arXiv:1203.4218](#)].
- [11] A. Crivellin, L. Hofer, and U. Nierste, *The MSSM with a softly broken  $U(2)^3$  flavor symmetry*, [arXiv:1111.0246](#).
- [12] A. Crivellin, L. Hofer, U. Nierste, and D. Scherer, *Phenomenological consequences of radiative flavor violation in the MSSM*, *Phys.Rev.* **D84** (2011) 035030, [[arXiv:1105.2818](#)].
- [13] A. Crivellin and U. Nierste, *Supersymmetric renormalisation of the CKM matrix and new constraints on the squark mass matrices*, *Phys.Rev.* **D79** (2009) 035018, [[arXiv:0810.1613](#)].
- [14] A. Pomarol and D. Tommasini, *Horizontal symmetries for the supersymmetric flavor problem*, *Nucl.Phys.* **B466** (1996) 3–24, [[hep-ph/9507462](#)].
- [15] R. Barbieri, G. Dvali, and L. J. Hall, *Predictions from a  $U(2)$  flavor symmetry in supersymmetric theories*, *Phys.Lett.* **B377** (1996) 76–82, [[hep-ph/9512388](#)].
- [16] R. Barbieri, D. Buttazzo, F. Sala, and D. M. Straub, *Less Minimal Flavour Violation*, [arXiv:1206.1327](#).

- 
- [17] Z. Ligeti, M. Papucci, G. Perez, and J. Zupan, *Implications of the dimuon CP asymmetry in  $B_{d,s}$  decays*, *Phys.Rev.Lett.* **105** (2010) 131601, [arXiv:1006.0432].
- [18] K. Blum, Y. Hochberg, and Y. Nir, *Implications of large dimuon CP asymmetry in  $B_{d,s}$  decays on minimal flavor violation with low  $\tan \beta$* , *JHEP* **1009** (2010) 035, [arXiv:1007.1872].
- [19] **Particle Data Group** Collaboration, K. Nakamura *et. al.*, *Review of particle physics*, *J.Phys.G* **G37** (2010) 075021.
- [20] P. Clarke, *Results on cp violation in  $b_s$  mixing*, .  
<http://cdsweb.cern.ch/record/1429149/files/LHCb-TALK-2012-029.pdf>.
- [21] J. Laiho, E. Lunghi, and R. S. Van de Water, *Lattice QCD inputs to the CKM unitarity triangle analysis*, *Phys. Rev.* **D81** (2010) 034503, [arXiv:0910.2928].  
Updates available on <http://latticeaverages.org/>.
- [22] G. Ricciardi, *Brief review on semileptonic B decays*, arXiv:1209.1407.
- [23] W. Altmannshofer, P. Paradisi, and D. M. Straub, *Model-Independent Constraints on New Physics in  $b \rightarrow s\gamma$  Transitions*, *JHEP* **1204** (2012) 008, [arXiv:1111.1257].
- [24] W. Altmannshofer and D. M. Straub, *Cornering New Physics in  $b \rightarrow s\gamma$  Transitions*, *JHEP* **1208** (2012) 121, [arXiv:1206.0273].
- [25] F. Botella, G. Branco, and M. Nebot, *The Hunt for New Physics in the Flavour Sector with up vector-like quarks*, arXiv:1207.4440.
- [26] G. Altarelli, F. Feruglio, and L. Merlo, *Tri-Bimaximal Neutrino Mixing and Discrete Flavour Symmetries*, arXiv:1205.5133.
- [27] G. Altarelli, F. Feruglio, L. Merlo, and E. Stamou, *Discrete Flavour Groups,  $\theta_{13}$  and Lepton Flavour Violation*, arXiv:1205.4670.
- [28] M. Bona *et. al.*, *SuperB: A High-Luminosity Asymmetric  $e^+e^-$  Super Flavor Factory. Conceptual Design Report*, arXiv:0709.0451.
- [29] M. Antonelli, D. M. Asner, D. A. Bauer, T. G. Becher, M. Beneke, *et. al.*, *Flavor Physics in the Quark Sector*, *Phys.Rept.* **494** (2010) 197–414, [arXiv:0907.5386].
- [30] M. Ciuchini and A. Stocchi, *Physics Opportunities at the Next Generation of Precision Flavor Physics*, *Ann.Rev.Nucl.Part.Sci.* **61** (2011) 491–517, [arXiv:1110.3920].
- [31] M. Blanke, A. J. Buras, K. Gemmler, and T. Heidsieck,  *$\Delta F = 2$  observables and  $B \rightarrow X_q\gamma$ ; in the Left-Right Asymmetric Model: Higgs particles striking back*, *JHEP* **1203** (2012) 024, [arXiv:1111.5014].

- 
- [32] A. J. Buras, M. V. Carlucci, L. Merlo, and E. Stamou, *Phenomenology of a Gauged  $SU(3)^3$  Flavour Model*, [arXiv:1112.4477](#).
- [33] J. Brod and M. Gorbahn, *Next-to-Next-to-Leading-Order Charm-Quark Contribution to the CP Violation Parameter  $\varepsilon_K$  and  $\Delta M_K$* , *Phys.Rev.Lett.* **108** (2012) 121801, [[arXiv:1108.2036](#)].
- [34] R. Fleischer, *Extracting  $\gamma$  from  $B(s/d) \rightarrow J/\psi K_S$  and  $B(d/s) \rightarrow D^+(d/s)D^-(d/s)$* , *Eur.Phys.J.* **C10** (1999) 299–306, [[hep-ph/9903455](#)].
- [35] M. Ciuchini, M. Pierini, and L. Silvestrini, *The Effect of penguins in the  $B_d \rightarrow J/\psi K^0$  CP asymmetry*, *Phys.Rev.Lett.* **95** (2005) 221804, [[hep-ph/0507290](#)].
- [36] M. Ciuchini, M. Pierini, and L. Silvestrini, *Theoretical uncertainty in  $\sin 2\beta$ : An Update*, [arXiv:1102.0392](#).
- [37] S. Faller, M. Jung, R. Fleischer, and T. Mannel, *The Golden Modes  $B^0 \rightarrow J/\psi K_{S,L}$  in the Era of Precision Flavour Physics*, *Phys.Rev.* **D79** (2009) 014030, [[arXiv:0809.0842](#)].
- [38] S. Faller, R. Fleischer, and T. Mannel, *Precision Physics with  $B_s^0 \rightarrow J/\psi \phi$  at the LHC: The Quest for New Physics*, *Phys.Rev.* **D79** (2009) 014005, [[arXiv:0810.4248](#)].
- [39] M. Jung and T. Mannel, *General Analysis of U-Spin Breaking in B Decays*, *Phys.Rev.* **D80** (2009) 116002, [[arXiv:0907.0117](#)].
- [40] K. De Bruyn, R. Fleischer, and P. Koppenburg, *Extracting gamma and Penguin Topologies through CP Violation in  $B_s^0 \rightarrow J/\psi K_S$* , *Eur.Phys.J.* **C70** (2010) 1025–1035, [[arXiv:1010.0089](#)].
- [41] A. J. Lenz, *A simple relation for  $B_s$  mixing*, *Phys.Rev.* **D84** (2011) 031501, [[arXiv:1106.3200](#)].
- [42] H. Boos, T. Mannel, and J. Reuter, *The Gold plated mode revisited:  $\sin(2\beta)$  and  $B^0 J/\psi K_S$  in the standard model*, *Phys.Rev.* **D70** (2004) 036006, [[hep-ph/0403085](#)].
- [43] H.-n. Li and S. Mishima, *Penguin pollution in the  $B^0 \rightarrow J/\psi K_S$  decay*, *JHEP* **0703** (2007) 009, [[hep-ph/0610120](#)].
- [44] M. Gronau and J. L. Rosner, *Doubly CKM-suppressed corrections to CP asymmetries in  $B^0 \rightarrow J/\psi K^0$* , *Phys.Lett.* **B672** (2009) 349–353, [[arXiv:0812.4796](#)].

- [45] M. Jung, *Determining weak phases from  $B \rightarrow J/\psi P$  decays*, arXiv:1206.2050.
- [46] A. J. Buras, M. V. Carlucci, S. Gori, and G. Isidori, *Higgs-mediated FCNCs: Natural Flavour Conservation vs. Minimal Flavour Violation*, *JHEP* **1010** (2010) 009, [arXiv:1005.5310].
- [47] A. J. Buras, G. Isidori, and P. Paradisi, *EDMs versus CPV in  $B_{s,d}$  mixing in two Higgs doublet models with MFV*, *Phys.Lett.* **B694** (2011) 402–409, [arXiv:1007.5291].
- [48] A. J. Buras, J. Girrbach, M. Nagai, and P. Paradisi, “2HDM<sub>MFV</sub> Facing Recent LHCb Data.”, *in preparation*.
- [49] K. De Bruyn, R. Fleischer, R. Knegjens, P. Koppenburg, M. Merk, *et. al.*, *Branching Ratio Measurements of  $B_s$  Decays*, *Phys.Rev.* **D86** (2012) 014027, [arXiv:1204.1735].
- [50] K. De Bruyn, R. Fleischer, R. Knegjens, P. Koppenburg, M. Merk, *et. al.*, *Probing New Physics via the  $B_s^0 \rightarrow \mu^+ \mu^-$  Effective Lifetime*, *Phys.Rev.Lett.* **109** (2012) 041801, [arXiv:1204.1737].
- [51] M. Blanke *et. al.*, *Particle antiparticle mixing,  $\varepsilon_K$ ,  $\Delta\Gamma_q$ ,  $A_{SL}^q$ ,  $A_{CP}(B_d \rightarrow \psi K_S)$ ,  $A_{CP}(B_s \rightarrow \psi\phi)$  and  $B \rightarrow X_{s,d}\gamma$  in the Littlest Higgs model with  $T$ -parity*, *JHEP* **12** (2006) 003, [hep-ph/0605214].
- [52] S. Herrlich and U. Nierste, *Enhancement of the  $K_L - K_S$  mass difference by short distance QCD corrections beyond leading logarithms*, *Nucl. Phys.* **B419** (1994) 292–322, [hep-ph/9310311].
- [53] S. Herrlich and U. Nierste, *Indirect CP violation in the neutral kaon system beyond leading logarithms*, *Phys. Rev.* **D52** (1995) 6505–6518, [hep-ph/9507262].
- [54] S. Herrlich and U. Nierste, *The Complete  $|\Delta S| = 2$  Hamiltonian in the Next-To-Leading Order*, *Nucl. Phys.* **B476** (1996) 27–88, [hep-ph/9604330].
- [55] A. J. Buras, M. Jamin, and P. H. Weisz, *Leading and next-to-leading QCD corrections to  $\varepsilon$  parameter and  $B^0 - \bar{B}^0$  mixing in the presence of a heavy top quark*, *Nucl. Phys.* **B347** (1990) 491–536.
- [56] J. Urban, F. Krauss, U. Jentschura, and G. Soff, *Next-to-leading order QCD corrections for the  $B^0 - \bar{B}^0$  mixing with an extended Higgs sector*, *Nucl. Phys.* **B523** (1998) 40–58, [hep-ph/9710245].
- [57] J. Brod and M. Gorbahn,  *$\varepsilon_K$  at Next-to-Next-to-Leading Order: The Charm-Top-Quark Contribution*, *Phys.Rev.* **D82** (2010) 094026, [arXiv:1007.0684].

- 
- [58] A. J. Buras, D. Guadagnoli, and G. Isidori, *On  $\epsilon_K$  beyond lowest order in the Operator Product Expansion*, *Phys.Lett.* **B688** (2010) 309–313, [[arXiv:1002.3612](#)].
- [59] M. Blanke and A. J. Buras, *Lower bounds on  $\Delta M_{s,d}$  from constrained minimal flavour violation*, *JHEP* **0705** (2007) 061, [[hep-ph/0610037](#)].
- [60] A. J. Buras and R. Buras, *A Lower bound on  $\sin 2\beta$  from minimal flavor violation*, *Phys.Lett.* **B501** (2001) 223–230, [[hep-ph/0008273](#)].
- [61] K. Chetyrkin, J. Kuhn, A. Maier, P. Maierhofer, P. Marquard, *et. al.*, *Charm and Bottom Quark Masses: An Update*, *Phys.Rev.* **D80** (2009) 074010, [[arXiv:0907.2110](#)].
- [62] **HPQCD Collaboration** Collaboration, I. Allison *et. al.*, *High-Precision Charm-Quark Mass from Current-Current Correlators in Lattice and Continuum QCD*, *Phys.Rev.* **D78** (2008) 054513, [[arXiv:0805.2999](#)].
- [63] **CDF Collaboration** Collaboration, A. Abulencia *et. al.*, *Observation of  $B_s^0 - \bar{B}_s^0$  Oscillations*, *Phys.Rev.Lett.* **97** (2006) 242003, [[hep-ex/0609040](#)].
- [64] **LHCb Collaboration** Collaboration, R. Aaij *et. al.*, *Measurement of the  $B_s^0 - \bar{B}_s^0$  oscillation frequency  $\Delta M_s$  in  $B_s^0 \rightarrow D_s^-(3)\pi$  decays*, *Phys.Lett.* **B709** (2012) 177–184, [[arXiv:1112.4311](#)].
- [65] **Belle Collaboration** Collaboration, I. Adachi *et. al.*, *Measurement of  $b \rightarrow \tau\nu$  with a hadronic tagging method using the full data sample of belle*, [arXiv:1208.4678](#).
- [66] C. Tarantino, *Flavor Lattice QCD in the Precision Era*, [arXiv:1210.0474](#).
- [67] C. Bouchard, E. Freeland, C. Bernard, A. El-Khadra, E. Gamiz, *et. al.*, *Neutral B mixing from 2 + 1 flavor lattice-QCD: the Standard Model and beyond*, [arXiv:1112.5642](#).
- [68] P. Boyle, N. Garron, and R. Hudspith, *Neutral kaon mixing beyond the standard model with  $n_f = 2 + 1$  chiral fermions*, [arXiv:1206.5737](#).
- [69] V. Bertone, N. Carrasco, M. Ciuchini, P. Dimopoulos, R. Frezzotti, *et. al.*, *Kaon Mixing Beyond the SM from  $N_f=2$  tmQCD and model independent constraints from the UTA*, [arXiv:1207.1287](#).
- [70] A. J. Buras, F. Parodi, and A. Stocchi, *The CKM matrix and the unitarity triangle: Another look*, *JHEP* **0301** (2003) 029, [[hep-ph/0207101](#)].
- [71] A. J. Buras, *Relations between  $\Delta M_{s,d}$  and  $B_{s,d} \rightarrow \mu^+\mu^-$  in models with minimal flavour violation*, *Phys. Lett.* **B566** (2003) 115–119, [[hep-ph/0303060](#)].

- 
- [72] **HPQCD Collaboration** Collaboration, J. Shigemitsu *et. al.*, *Recent results on B mixing and decay constants from HPQCD*, *PoS LAT2009* (2009) 251, [arXiv:0910.4131].
- [73] **LHCb collaboration** Collaboration, R. Aaij *et. al.*, *Strong constraints on the rare decays  $B_s \rightarrow \mu^+ \mu^-$  and  $B^0 \rightarrow \mu^+ \mu^-$* , arXiv:1203.4493.
- [74] **LHCb collaboration** Collaboration, R. Aaij *et. al.*, *First evidence for the decay  $B_s \rightarrow \mu^+ \mu^-$* , arXiv:1211.2674.
- [75] A. J. Buras, J. Girrbach, D. Guadagnoli, and G. Isidori, *On the Standard Model prediction for  $\mathcal{B}(B_{s,d} \rightarrow \mu^+ \mu^-)$* , arXiv:1208.0934.